Biosensors and Bioelectronics 86 (2016) 643–655

Contents lists available at ScienceDirect

Biosensors and Bioelectronics

journal homepage: www.elsevier.com/locate/bios

Reversibly monitoring oxidation and reduction events in living biological systems: Recent development of redox-responsive reversible NIR biosensors and their applications in *in vitro/in vivo* fluorescence imaging

Tian-shu Chu [a,d,*], Rui Lü [b], Bai-tong Liu [c,d]

[a] Institute for Computational Sciences and Engineering, Laboratory of New Fiber Materials and Modern Textile, The Growing Base for State Key Laboratory and College of Physics, Qingdao University, Qingdao, 266071 China
[b] Laboratory of Pathogenic Biology, Medical College, Qingdao University, Qingdao, 266071 China
[c] College of Chemical Science and Engineering, Qingdao University, Qingdao, 266071 China
[d] State Key Laboratory of Molecular Reaction Dynamics, Dalian Institute of Chemical Physics, Chinese Academy of Sciences, Dalian, 116023 People's Republic of China

ARTICLE INFO

Article history:
Received 24 March 2016
Received in revised form
25 June 2016
Accepted 11 July 2016
Available online 12 July 2016

Keywords:
Redox-responsive reversible NIR biosensor
Reactive oxygen species
Redox changes
In vitro/in vivo fluorescence imaging
Living cells and small animals

ABSTRACT

Reactive oxygen species (ROS) and changes in their redox cycles have great therapeutic potential for treating serious redox-related human diseases such as acute and chronic inflammation, diabetes, cancer and neurodegenerative disorders. This article presents a survey of the recently (2011–2016) developed NIR small-molecule biosensors for reversibly monitoring oxidation and reduction events in living cells and small animals through *in vitro/in vivo* fluorescence imaging. Emission and absorption profile, design strategy and fluorescence sensing mechanism, ROS selectivity and sensitivity, reversibility, ability of subcellular location and cytotoxicity are discussed for the NIR small-molecule biosensors capable of quantitatively, continuously and reversibly detecting transient ROS burst and redox changes at cellular level.

Contents

1. Introduction

The strict control over internal redox status is very important to the function and health of a biological system that lives in aerobic environments (Miller et al., 2007; Fruehauf et al., 2007; Droge, 2002; Finkel 2011; Wu, 2010; Wardman, 2007; Dickinson et al.,

* Corresponding author at: Institute for Computational Sciences and Engineering, Laboratory of New Fiber Materials and Modern Textile, The Growing Base for State Key Laboratory and College of Physics, Qingdao University, Qingdao 266071, China.
E-mail addresses: tschu@dicp.ac.cn, tschu008@163.com (T.-s. Chu).

http://dx.doi.org/10.1016/j.bios.2016.07.039
0956-5663/

2010). Being the second messengers in a biological process, reactive oxygen species (ROS) (some overlapped with reactive nitrogen species (RNS)) in cellular compartments form the unique biological oxidation and reduction cycles mediating cellular signal transduction and homeostasis regulation (Dickinson and Chang, 2011; Shahrokhian, 2001; Yap et al., 2007; Chen et al., 2010). Unregulated generation of ROS will cause oxidative damage to proteins, lipids and nucleic acids, which is connecting to serious human diseases such as diabetes, cancer and neurodegenerative disease disorders including Alzheimer's disease and Parkinson's disease where age is a risk factor (Miller et al., 2007; Wardman, 2007; Dickinson et al., 2010; Dickinson and Chang, 2011; Lu et al., 2004; Balaban et al., 2005; Gunnlaugsson et al., 2006; Que et al., 2008; Schulz et al., 2000). As a result, precise measurement of ROS and real-time monitoring their redox homeostasis changes should have broad physiological and pathological perspective.

Many technology and tools have been developed and applied to detecting transient ROS burst and relevant oxidation and reduction events in living systems. Due to its greater sensitivity, more convenience and less invasiveness, fluorescence imaging becomes the most favorite choice for biological imaging (Yang et al., 2013). Especially, *in vivo* fluorescence imaging which uses a sensitive camera to detect fluorescence emission from fluorophores in whole-body living small animals (Rao et al., 2007) prefers near infrared (NIR) light (650–900 nm) due to the multifaceted advantages of the NIR imaging, including deep tissue penetration, minimum photodamage and minimum background autofluorescence interference.

Recently, fluorescence imaging with redox-responsive fluorescent biosensor has become one of the most powerful tools for establishing a real-time visualization of the various stages of oxidative signaling, stress, or repair in living systems. Today, the rapid development in the design and synthesis of fluorescent biosensors facilitates the fast growing of redox-sensitive fluorescent biosensors (Miller et al., 2007; Benniston et al., 2008; Yamada et al., 2008; Kierat et al., 2010; Hirosawa et al., 2012; Reddie et al., 2012; Wang et al., 2013a, 2013a, 2013b; Lou et al., 2013a, 2013a, 2014, 2013b, 2015; Liu and Wu, 2013; Zhang et al., 2013; Manjare et al., 2014a, 2014b, 2014c; Yu et al., 2012a, 2012b, 2011, 2013, 2012c, 2012d; Koide et al., 2012; Takahashi et al., 2012; Xu et al., 2011, 2013; Kundu et al., 2009; Li et al., 2015; Narayanaswamy et al., 2016; Nie et al., 2016; Yin et al., 2015). Generally, these redox-sensitive small-molecule biosensors can be categorized into ultraviolet (UV)–visible and NIR biosensors, or alternatively into irreversible and reversible biosensors. Compared with the UV–visible biosensors whose fluorescence excitation and emission locate in the UV or visible region (Miller et al., 2007; Benniston et al., 2008; Yamada et al., 2008; Kierat et al., 2010; Hirosawa et al., 2012; Reddie et al., 2012; Wang et al., 2013a, 2013b; Lou et al., 2013a, 2013b, 2014, 2013c, 2015; Liu and Wu, 2013; Zhang et al., 2013; Manjare et al., 2014a, 2014b, 2014c; Yu et al., 2012a, 2012b), the NIR biosensors (Koide et al., 2012; Takahashi et al., 2012; Yu et al., 2011, 2013, 2012c, 2012d; Xu et al., 2011, 2013; Wang et al., 2013b; Kundu et al., 2009; Li et al., 2015; Narayanaswamy et al., 2016; Nie et al., 2016; Yin et al., 2015) are more optimal for *in vivo* fluorescence imaging due to the afore-mentioned reasons. In contrast to the irreversible biosensors which are limited in their usefulness, the reversible biosensors capable of cycling back and forth through continuous oxidation and reduction events have the excellent ability to distinguish and sense the transient bursts in ROS production within cells and thus allow for visualizing the changes in redox homeostasis in living systems through fluorescence imaging. Further, compared with the genetic reporters for ROS which can also allow for the reversible detection of ROS, fluorescent small-molecule ROS biosensors are sometimes more convenient due to the rather complicated nature of genetic manipulation (Woolley et al., 2013).

There have quite a few reviews on NIR fluorescent probes and ROS probes. For example, in 2014, Yoon and Shin and coworkers published a nice review on "Recent progress in the development of near-infrared fluorescent probes for bioimaging applications" that highlights the recent advances (2010–2013) in the development and applications of NIR fluorescent probes including ROS/RNS-responsive probes (Guo et al., 2014). The good review published by Cotter and coworkers in 2013 discusses the improvements in methodologies and technologies that have improved the specificity, localization and sensitivity of the ROS probes (Woolley et al., 2013). In 2012, Chang and coworkers published another nice review which presents a survey of tools and tactics for using reaction-based small-molecule fluorescent probes to detect biologically important chemical analytes including ROS (Chan et al., 2012).

In this article, we conduct a survey on the recently (2011–2016) developed redox-sensitive reversible NIR fluorescent small-molecule biosensors which can continuously and reversibly monitor the oxidation and reduction events in living cells and small animals through fluorescence imaging (Yu et al., 2011, 2013, 2012c, 2012d; Xu et al., 2011, 2013; Wang et al., 2013c; Takahashi et al., 2012; Koide et al., 2012; Nie et al., 2016). For these developed NIR fluorescent biosensors, special attention is given to their spectroscopic property, design strategy and fluorescence sensing mechanism, ROS selectivity and sensitivity, reversibility, capability of subcellular location, cytotoxicity, and applications in *in vitro/in vivo* fluorescence imaging. Finally, we summarize the features of the NIR small-molecule biosensors recently developed for reversibly monitoring redox changes and give suggestions about the future design and applications of redox-responsive reversible NIR small-molecule biosensors.

2. $ONOO^-$-sensitive NIR biosensors: reversibly monitoring the redox cycles between peroxynitrite and thiols

As a highly RNS or ROS, the peroxynitrite ($ONOO^-$) plays significant role in living biological systems because of the double-edged character of ROS: a well-controlled level of $ONOO^-$ is good at driving and mediating cellular functions whereas a high level of $ONOO^-$ can cause oxidative (or nitrosative) damage and lead to many serious redox-related diseases.

Three developed reversible NIR biosensors all showed great specificity, fast response, and high sensitivity towards $ONOO^-$ against other ROS/RNS (or other biologically relevant species) *in vitro/in vivo*. The switch on-off NIR biosensor Cy-PSe, in Fig. 1, from Han's laboratory (Yu et al., 2011) was developed and based on the organoselenium compound of monoselenides (a major glutathione peroxidase (GPx) mimic) (Nascimento et al., 2012). It features a 4-(phenylselanyl)aniline fluorescent modulator with specific and sensitive responses to $ONOO^-$ and a NIR fluorescent heptamethine cyanine (Cy) dye. This biosensor shows maximum absorption and emission at 758 nm and 775–800 nm, respectively. The fluorescence is switched on upon detection of $ONOO^-$ with an increase factor of 23.3-fold but is switched off when responds to the main *in vivo* antioxidants glutathione (GSH) and L-cysteine. Density functional theory (DFT) and time-dependent density functional theory (TD-DFT) study revealed that the fast photo-induced electron transfer (PET) mechanism on the excited state between the modulator and the heptamethine cyanine dye is responsible for the fluorescence quenching while the PET is blocked with the Se oxidation by $ONOO^-$ to cause the fluorescence emission to be switched on. Being applied in *in vitro* confocal fluorescence imaging, biosensor Cy-PSe successfully and reversibly monitored the multiple redox cycles between $ONOO^-$ oxidative stress and GSH reduction in the mouse macrophage cell line RAW264.7 (see Fig. 1).

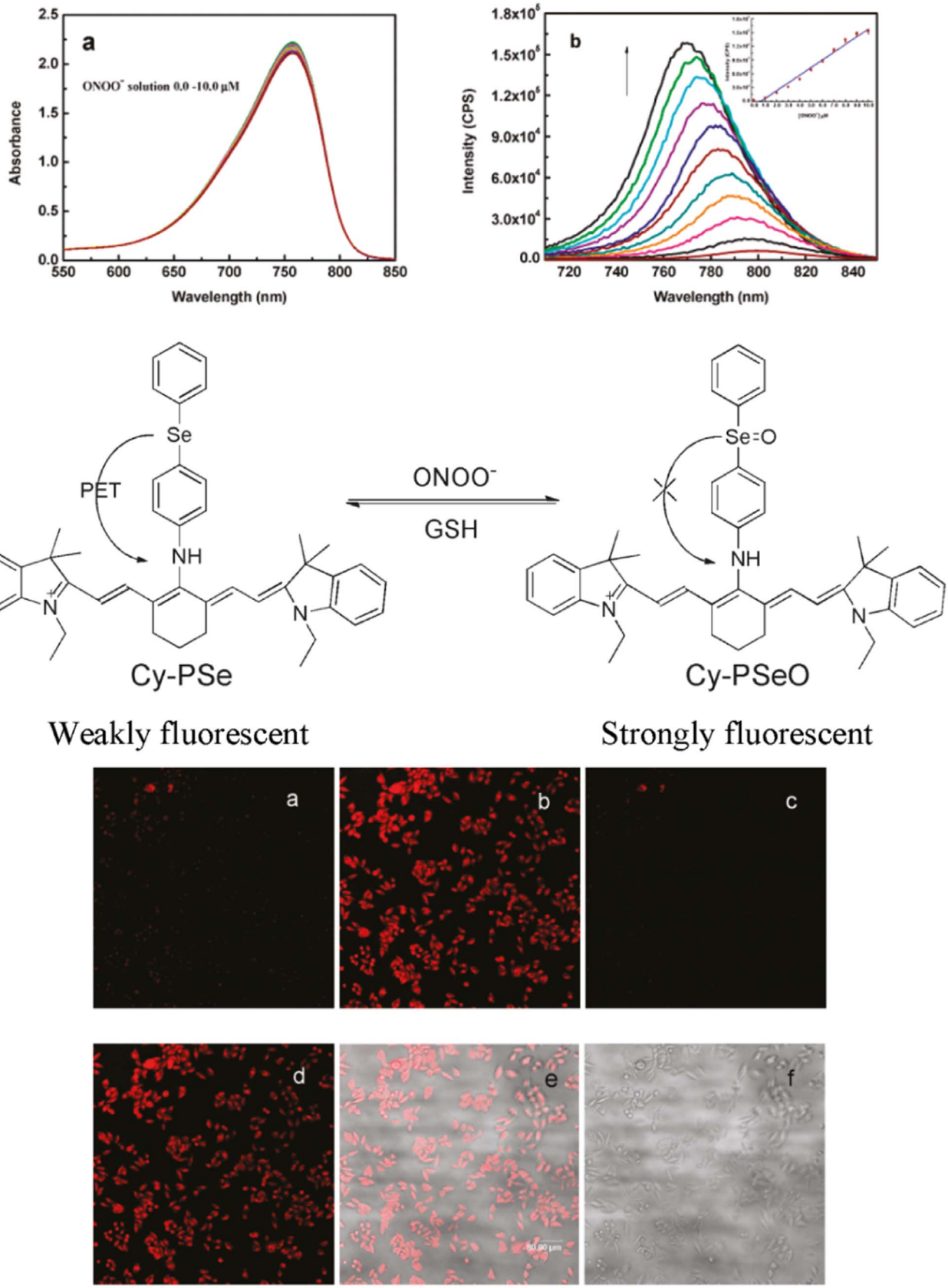

Fig. 1. Biosensor Cy-PSe and its oxidized product Cy-PSeO, its spectroscopic features under simulated physiological conditions (pH 7.40, 0.1 M PBS, 10.0 μM Cy-PSe) and *in vitro* confocal fluorescence imaging of reversible redox cycles between $ONOO^-$/thiols in living RAW264.7 cells. [From Yu et al. (2011)].

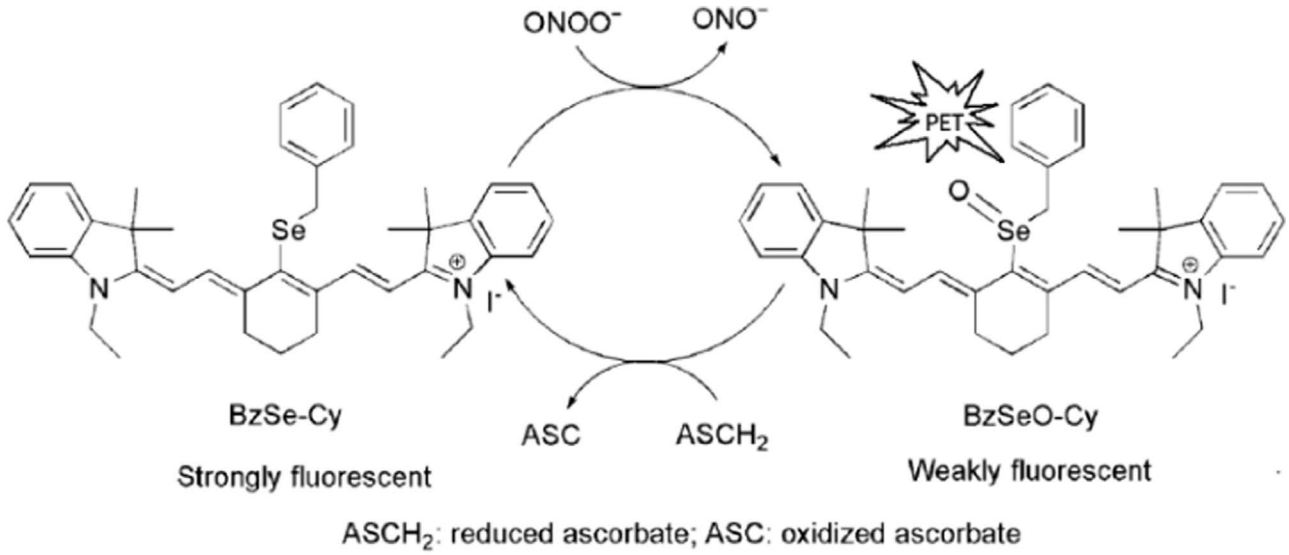

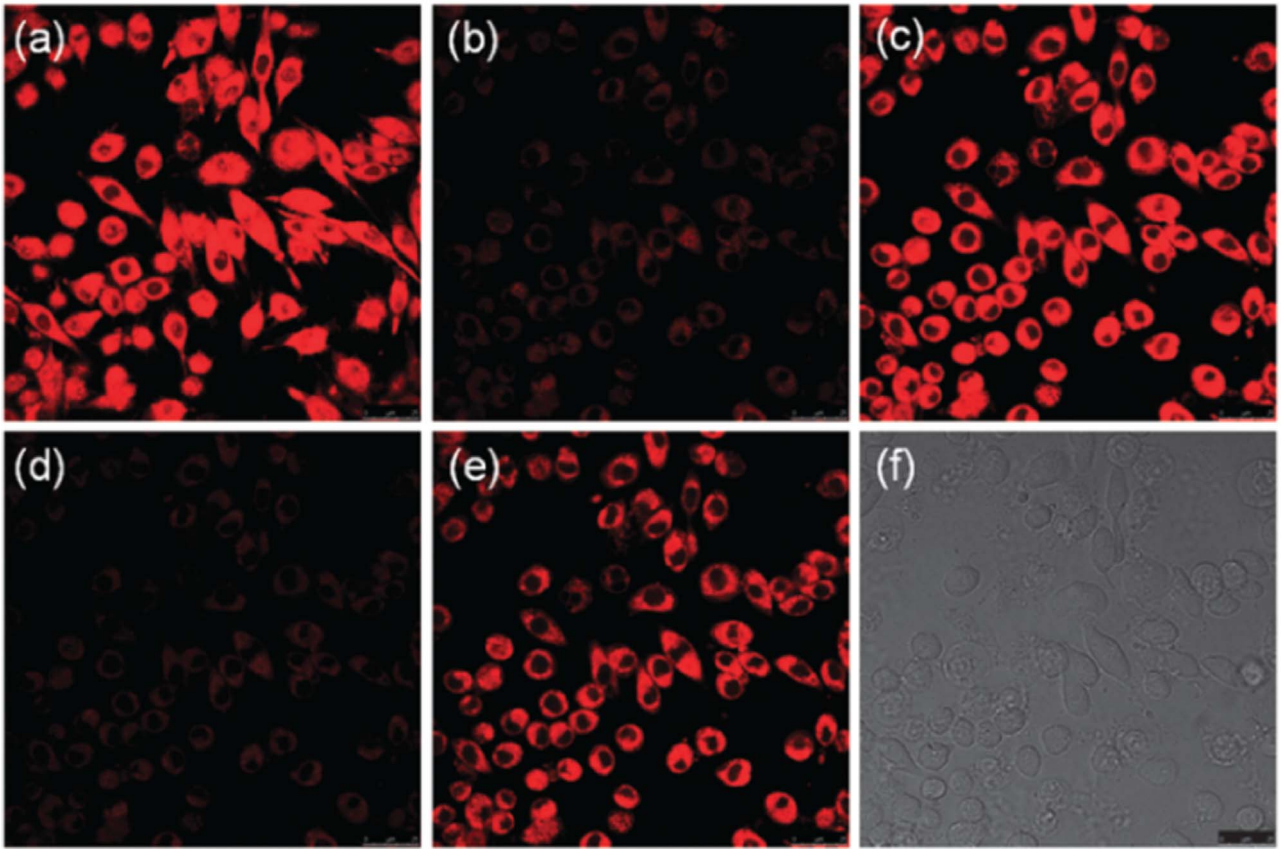

Fig. 2. Biosensor BzSe-Cy and its oxidized product BzSeO-Cy, and *in vitro* confocal fluorescence imaging of the multiple redox cycles between $ONOO^-/ASCH_2$ in living RAW264.7 cells at 37 °C. [From Xu et al. (2011)].

Biosensor BzSe-Cy, in Fig. 2, from Tang's laboratory (Xu et al., 2011) was developed and based also on the organoselenium compound (Nascimento et al., 2012) of monoselenides. It contains the heptamethine cyanine dye as the NIR fluorophore and the divalent selenium as a redox-responsive group. BzSe-Cy emits NIR light with a maximum emission around 795 nm and its fluorescence emission is switched "off" and "on" when it responds to $ONOO^-$ and the antioxidant ascorbate ($ASCH_2$), respectively. The fluorescent intensity decreases with a factor of 5-fold upon detection of $ONOO^-$ and the weak fluorescent signal is due to the PET mechanism in BzSeO-Cy, that is, the oxidized product of BzSe-Cy by $ONOO^-$. BzSe-Cy was also demonstrated to be effective for the reversible and real-time monitoring of the redox changes between $ONOO^-$ oxidative stress and ascorbate reductive repair in RAW264.7 cells with confocal laser scanning microscopy.

Biosensor Cy-NTe, in Fig. 3, also from Han's group (Yu et al., 2013) was a tellurium-based compound (Ba et al., 2010), in which the NIR fluorescent heptamethine cyanine dye acts as the signal transducer and the 2-(phenyltellanyl)benzohydrazide (NTe) serves as fluorescent modulator. Cy-NTe shows absorption peak and emission peak at 793 nm and 820 nm respectively and has the $ONOO^-$ detection limit of 9.17×10^{-7} M in potassium phosphate solution. The fluorescent

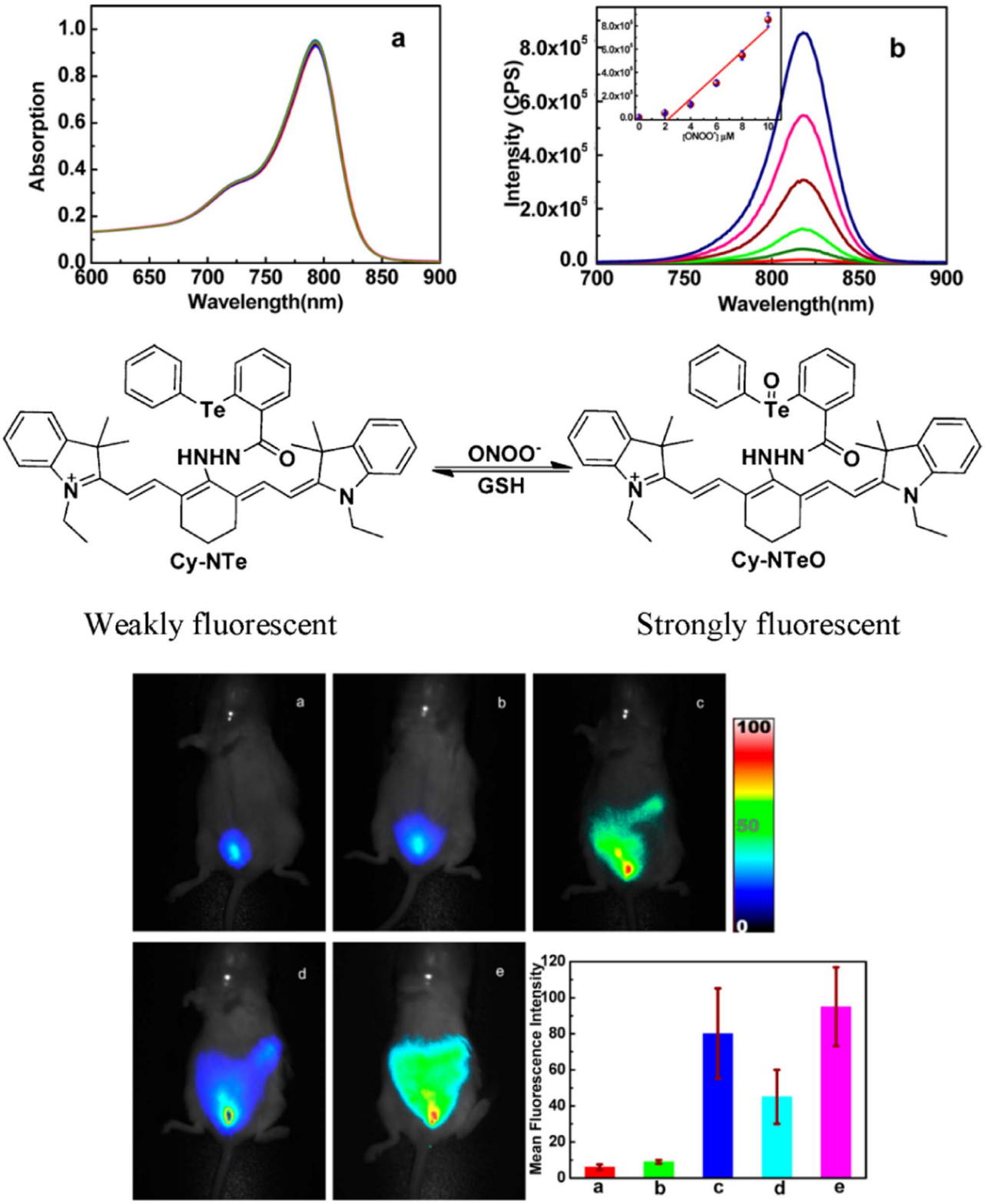

Fig. 3. Biosensor Cy-NTe and its oxidized product Cy-NTeO, its spectroscopic features under simulated physiological conditions (50 mM PBS pH 7.4, 10 μM) and *in vivo* fluorescence imaging of the reversible redox cycles between $ONOO^-$ and GSH in peritoneal cavity of the mice BALB/c. [From Yu et al. (2013)].

intensity of Cy-NTe increases upon the detection of $ONOO^-$ (*i.e.*, quantum yield changes from 0.0032 to 0.0431), the mechanism of which is due to the blocking of the fast PET process by the selective oxidation of the tellurium atom by $ONOO^-$. This biosensor allowed for the real-time imaging of the redox changes in living cells and animals. Especially, the *in vivo* fluorescent imaging of redox cycles between mitochondrial peroxynitrite and GSH in peritoneal cavity of the mice BALB/c under different treatment conditions has highlighted the enough sensitivity of this biosensor in visualizing the $ONOO^-$ redox reversibility in living animals, which can be indicated from the data about the quantification of mean fluorescence intensity of each treatment condition (see Fig. 3).

The three biosensors all showed good ability to target and retain in the mitochondria (*i.e.*, a major cellular source of ROS) and are low toxicity to the cultured cell lines (see the bright-field image (f) in Figs. 1–2). The reversibility of the three biosensors was demonstrated by that the reversible oxidation-reduction cycles can be repeated at least 5 times with no loss of fluorescence intensity, 8 times with no loss of intensity and 5 times with a moderate loss of intensity. Among the three biosensors, Cy-PSe has the fast respond speed to the $ONOO^-$ changes within 8 min, and the other two biosensors BzSe-Cy and Cy-NTe respond within 30 and 10 min, respectively.

Recently, based on the 2-(2′- hydroxyphenyl)benzothiazole (BT) fluorophores, a two-photon "switch-on" biosensor NP3 (Li et al., 2015) was synthesized in Hu's laboratory by switching the hydroxyl group of BT to N-methyl-*p*-hydroxyaniline and then installing electron-donating groups to the *p*-hydroxyaniline ring through Mills reaction. NP3 showed obvious fluorescent enhancement with an increase factor of 600-fold upon the detection of $ONOO^-$ and was demonstrated to be very effective for real-time imaging of $ONOO^-$ generation in both living cells and animals. In particular, NP3 has realized the real-time imaging of endogenous peroxynitrite formation after brain microvessel injury in living mice. The advantages of NP3 lie in its two-photon excitability, low detection limit of 5.0 nM, high temporal and spatial resolution, and good blood-brain barrier penetrability. Especially, two-photon biosensors are compatible with two-photon microscopy offering longer observation time, less photodamage, deeper tissue penetration and local excitation. But NP3 is not reversible.

3. HBrO-sensitive NIR biosensors: reversible monitoring the multiple redox cycles between HBrO and ascorbic acid and between HBrO and H_2S

In vivo excessive production of hypobromous acid (HBrO) can cause tissue damage and thus leads to many diseases like asthma, cardiovascular diseases, arthritis and cancers. Recently, Han and coworkers devised and synthesized two NIR biosensors Cy-TemOH (Yu et al., 2012c) and diMPhSe-BOD (Wang et al., 2013c) which only respond to HBrO, as shown in Fig. 4. These two biosensors were demonstrated to be effective for reversibly monitoring the multiple redox cycles between hypobromous acid and ascorbic acid, and between hypobromous acid and hydrogen sulfide (H_2S), respectively, in the mouse macrophage living RAW264.7 cells.

In Cy-TemOH, the heptamethine cyanine platform is acting as the fluorophore and the integrated 4-hydroxylamino-2,2,6,6-tetramethylpiperidine-N-oxyl (TemOH) moiety is acting as the fluorescent modulator that responses to the redox changes of HBrO. Cy-TemOH showed maximum absorption and emission at 702 nm and 755 nm, respectively, and its fluorescence quantum yield reduced to 0.02 upon the detection of HBrO. As known, the reaction with HBrO triggers the chemoselective oxidation of hydroxylamine to oxoammonium cations (Oam) (Ishii et al., 2011), and the TemOH-fluorophores have strong fluorescent emission while the Oam-fluorophores have faint fluorescent emission. Based on the DFT/TD-DFT calculations, the sensing mechanism of Cy-TemOH is clarified to be a donor-excited PET (d-PET) mechanism between the excited-state fluorophore and Oam, and once the d-PET is prevented by the Oam reduction, the biosensor can emit strong red fluorescence.

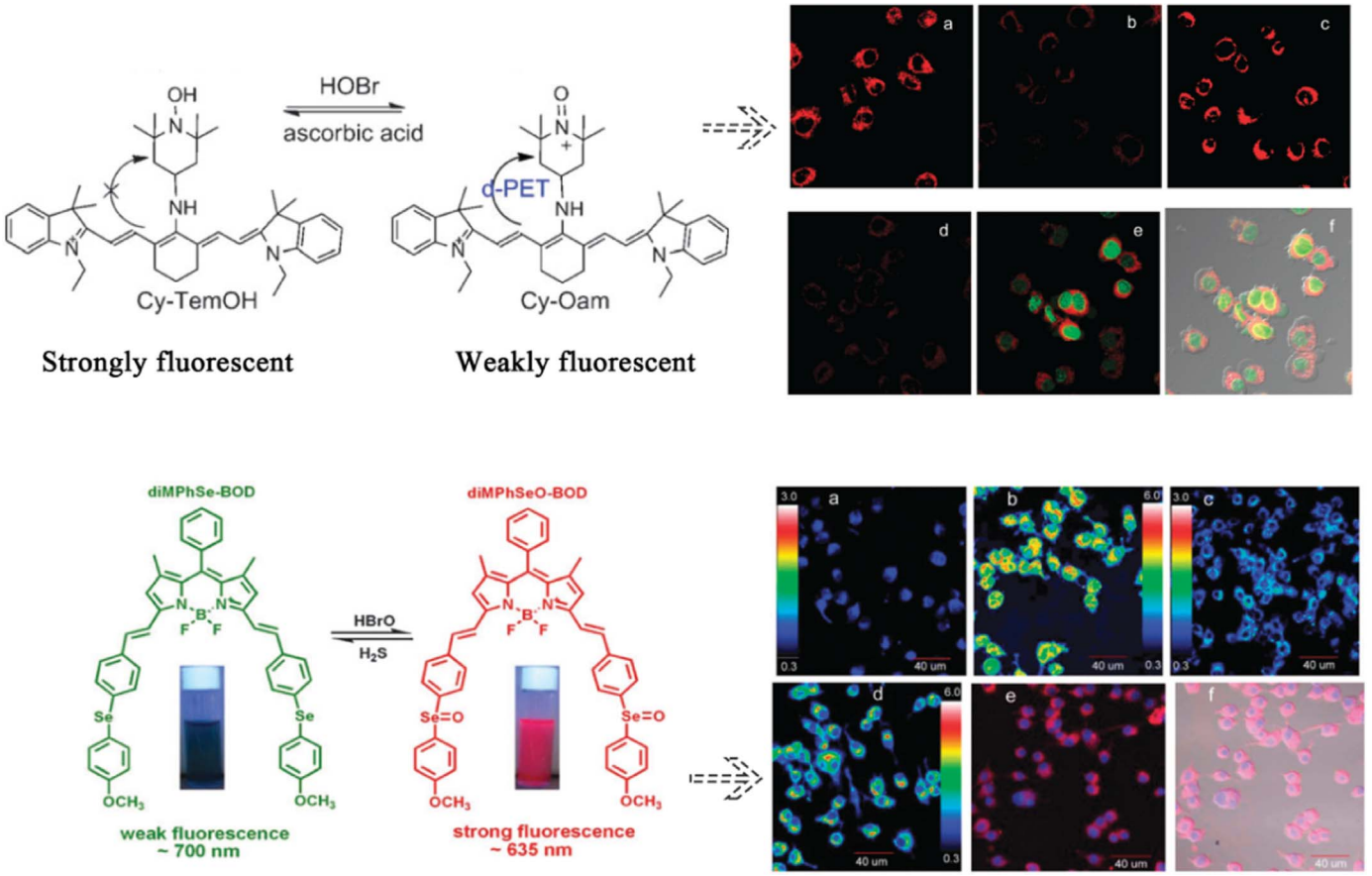

Fig. 4. Biosensor Cy-TemOH and the real-time monitoring of the multiple redox cycles between HBrO and ascorbic acid in the mouse macrophage living RAW264.7 cells by confocal microscopy imaging with Cy-TemOH [From Yu et al. (2012c)]. Biosensor diMPhSe-BOD and its oxidized product diMPhSeO-BOD, and the real-time ratiometric visualization of the multiple redox cycles between HBrO and H_2S in living RAW264.7 cells by confocal fluorescence imaging with diMPhSeO-BOD [From Wang et al. (2013c)].

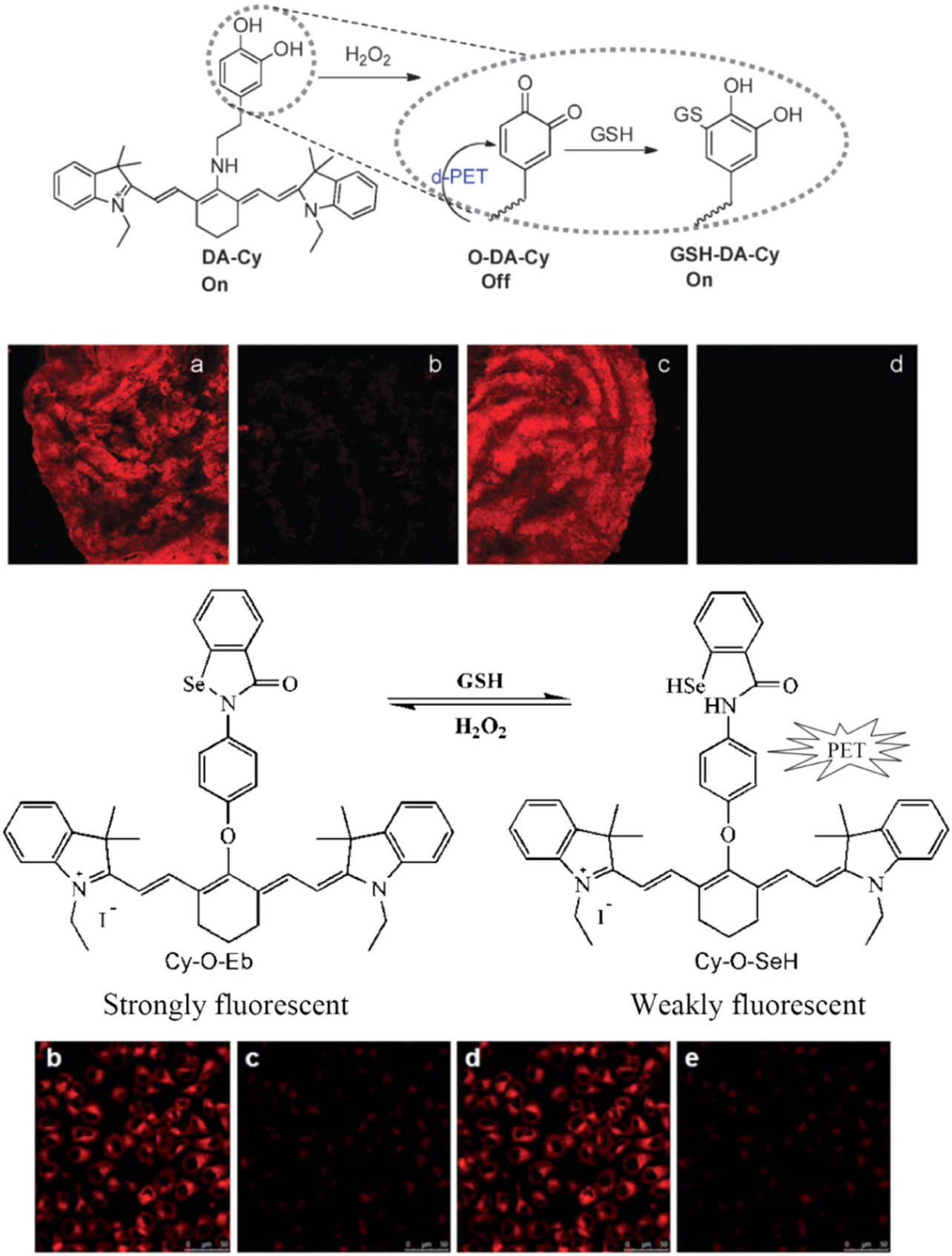

Fig. 5. Biosensor DA–Cy and the reversible sensing of H_2O_2 oxidative stress and thiols repair in the fresh rat hippocampus tissues by confocal microscopy and DA-Cy [From Yu et al. (2012d)]. Biosensor Cy-O-Eb and monitoring the redox changes between H_2O_2 and GSH in living HepG2 cells by confocal laser scanning microscopy [From Xu et al. (2013)].

Biosensor diMPhSe-BOD was based on Se-BODIPY with the BODIPY dye as the fluorophore and the 4-methyoxylphenylselenide (MPhSe) as the modulator. Here, the modulator was integrated into the fluorescent platform through a styrene bridge. The diMPhSe-BOD showed a maximum (weak) emission at 711 nm and its NIR profiles are due to the strong electron-donating properties of the Se group. Upon the detection of HBrO, a new emission band centered at 635 nm appears with rapidly increased intensity (230-fold). Thus, diMPhSe-BOD is actually a ratiometric type of NIR biosensor, demonstrating a linear relationship between the fluorescent intensity ratios F_{635}/F_{711} and the HBrO concentrations. This intensity ratio F_{635}/F_{711} increases by a factor of 118-fold upon HBrO detection. As for its sensing mechanism, the heavy atom effects (Kurishita et al., 2010) are responsible for the weak fluorescence emission at 711 nm, and after the "selenide" is oxidized to "selenoxide" by HBrO, the weaker electron donating ability of "selenoxide" has shortened the donor–acceptor π–conjugated system and causes the strong fluorescence emission at 635 nm.

The subcellular location of the two biosensors was demonstrated to be in the cytoplasm of the living cells. Their redox cycle profiles (*i.e.*, reversibility) demonstrated a moderate loss in fluorescent intensity during 3 oxidation-reduction cycles for Cy-TemOH and a moderate 18% decrement in intensity ratio during 5 cycles for diMPhSe-BOD. The respond time to HBrO of Cy-TemOH and diMPhSe-BOD is within 30 min and within 3 min, respectively. Compared with Cy-TemOH, diMPhSe-BOD has an advantage of ratiometric sensing which can cancel out the variability arising from environmental factors. In addition, the bright-field images confirmed the biosensors' low cytotoxicity to the living cells.

4. H_2O_2-sensitive NIR biosensors: reversibly monitoring the redox changes between hydrogen peroxide and thiols

The hydrogen peroxide (H_2O_2) is also an important ROS species and has a rather high cellular concentration. It usually has close relation to those cellular processes like the respiratory chain activity and the b-oxidation of fatty acids, *etc.* The *in vivo* excessive concentration of hydrogen peroxide can cause oxidative stress that connects to neurodegenerative and cardiovascular diseases, cancers, *etc.*

As shown in Fig. 5, two reversible biosensors DA–Cy (Yu et al., 2012d) and Cy-O-Eb (Xu et al., 2013) respond only to H_2O_2 at physiologically relevant levels and allow for real-time monitoring of its multiple redox cycles in living cells (Baker, 2010), tissues and living animals. The "on-off-on" biosensor DA–Cy was developed in Han's laboratory by integrating a dopamine (DA) unit into a cyanine scaffold via central substitution, which showed a major absorption maximum at 630 nm and a fluorescent maximum at 755 nm, respectively. Upon detection of H_2O_2, its fluorescence intensity decreases and switches off, but the fluorescence is gradually switched on with the GSH reduction. Normally, reaction with H_2O_2 oxidized DA to DA-o-quinone (Shen et al., 1996). Thus, when the biosensor is oxidized, the fluorescence is switched off due to the d-PET mechanism between DA-o-quinone and the cyanine fluorophore, while the fluorescence re-emits when the d-PET is prevented by the GSH reduction. Biosensor DA–Cy was demonstrated to be effective for image monitoring the reversible H_2O_2 oxidative stress and GSH reducing repair in living HL-7702 and HepG2 and RAW264.7 cell lines, and confocal microscopy experiments also demonstrated its unique ability in reversibly sensing the process of H_2O_2 oxidative stress and thiols repair at 150 μm in fresh rat hippocampus tissue.

Biosensor Cy-O-Eb was developed by integrating the ebselen (Eb) moiety (a modulator with unique response to H_2O_2/GSH) into the heptamethine cyanine fluorophore platform. It showed maximum absorption and maximum emission at 768 nm and 794 nm, respectively. The fluorescence intensity decreased rapidly with the GSH reduction, and the intensity recovered and increased rapidly upon the detection of H_2O_2. As for the sensing mechanism, the reaction with GSH converted Cy-O-Eb to the reduced Cy-O-SeH, and the PET mechanism in Cy-O-SeH makes it weakly fluorescent. With confocal laser scanning microscopy, Cy-O-Eb successfully achieved the real-time imaging of redox cycles in living HepG2 cells (Fig. 5), redox changes during L-buthionine sulfoximine (BSO)-induced apoptosis in HepG2 and HL7702 cells and *in vivo* H_2O_2 changes at the wound margin in zebrafish larvae. Moreover, the real-time monitoring during the BSO-induced apoptosis revealed that cancer cell apoptosis has reversibility and the reversal can be promoted by the recovery of intracellular reduced microenvironment.

DA–Cy is capable to locate in the cytoplasm of the living cells and has a good permeability in the tissues. Cy-O-Eb is targetable to mitochondria with good reversibility demonstrated by that the reversible redox cycle can be repeated more than four times with no loss of fluorescent intensity. They both have low cytotoxicity to living cells and respond rapidly to H_2O_2 within 9 min and 5 min, respectively.

Recently, Govindaraju and coworkers (Narayanaswamy et al., 2016) reported a stimuli-responsive NIR biosensor which allowed for measuring *in vitro* levels of H_2O_2. The switch-on biosensor QCy-BA ⊂ DNA was based on phenyl boronic acid-functionalized quinone-cyanine (QCy-BA) in combination with AT-rich exogenous or endogenous nuclear DNA. This approach of combining DNA fluorescence biosensor with stimuli-responsive appendages is interesting and useful to develop new stimuli-responsive biosensors. However, QCy-BA ⊂ DNA is not a reversible NIR biosensor.

5. O_2-sensitive NIR biosensor: reversibly monitoring hypoxia-normoxia cycles in living cells

Diseases such as cardiovascular diseases, tumors and stroke all related to hypoxia. Shown in Fig. 6, the reversible biosensor RHyCy5 was developed in Hanaoka's laboratory (Takahashi et al., 2012) for real-time monitoring of the repeated hypoxia-normoxia cycles in living cells. Its development strategy utilized the Förster resonance energy transfer (FRET) mechanism, *i.e.*, in RHyCy5, QSY-21 (darker quencher of fluorescence in NIR region) acts as FRET acceptor and cyanine dye Cy5 acts as FRET donor. The maximum absorption and maximum emission of the biosensor is located at 660 nm and 650 nm, respectively. RHyCy5 showed weak fluorescence under normoxia, but its fluorescence intensity increased with a factor of (7 − 8)-fold under hypoxia.

The sensing mechanism of RHyCy5 is associated with the redox behavior of QSY-21. Under hypoxia, QSY-21 can be one-electron reduced to its radical form QSY-21-radical (see Fig. 6), and this reduced radical form undergoes rapid oxidation when exposed to air. Such rapid oxidation and the large separation between Cy5 and QSY-21 in RHyCy5 caused the decreased fluorescence of the biosensor from hypoxia to normoxia, instead of the fluorescence quenching of the Cy5 fluorophores. The strong fluorescence under hypoxia is due to no FRET in RHyCy5-radical. In combination with fluorescence confocal microscopy, biosensor RHyCy5 has successfully monitored the repeated cycles of hypoxia-normoxia in living A549 cells within 5 h. In addition, the biosensor responds to hypoxia and normoxia within 1 h and 10 min, respectively. The other features of the biosensor such as reversible profile, ability of subcellular location, cytotoxicity were not reported.

6. ROS-sensitive NIR biosensors: reversibly monitoring the redox cycles between ROS and GSH

Generally, multiple ROS of H_2O_2, $O_2^{\cdot -}$, ·OH, O_2, and HOCl coexist *in vivo* and transformation among these ROS usually occurs in

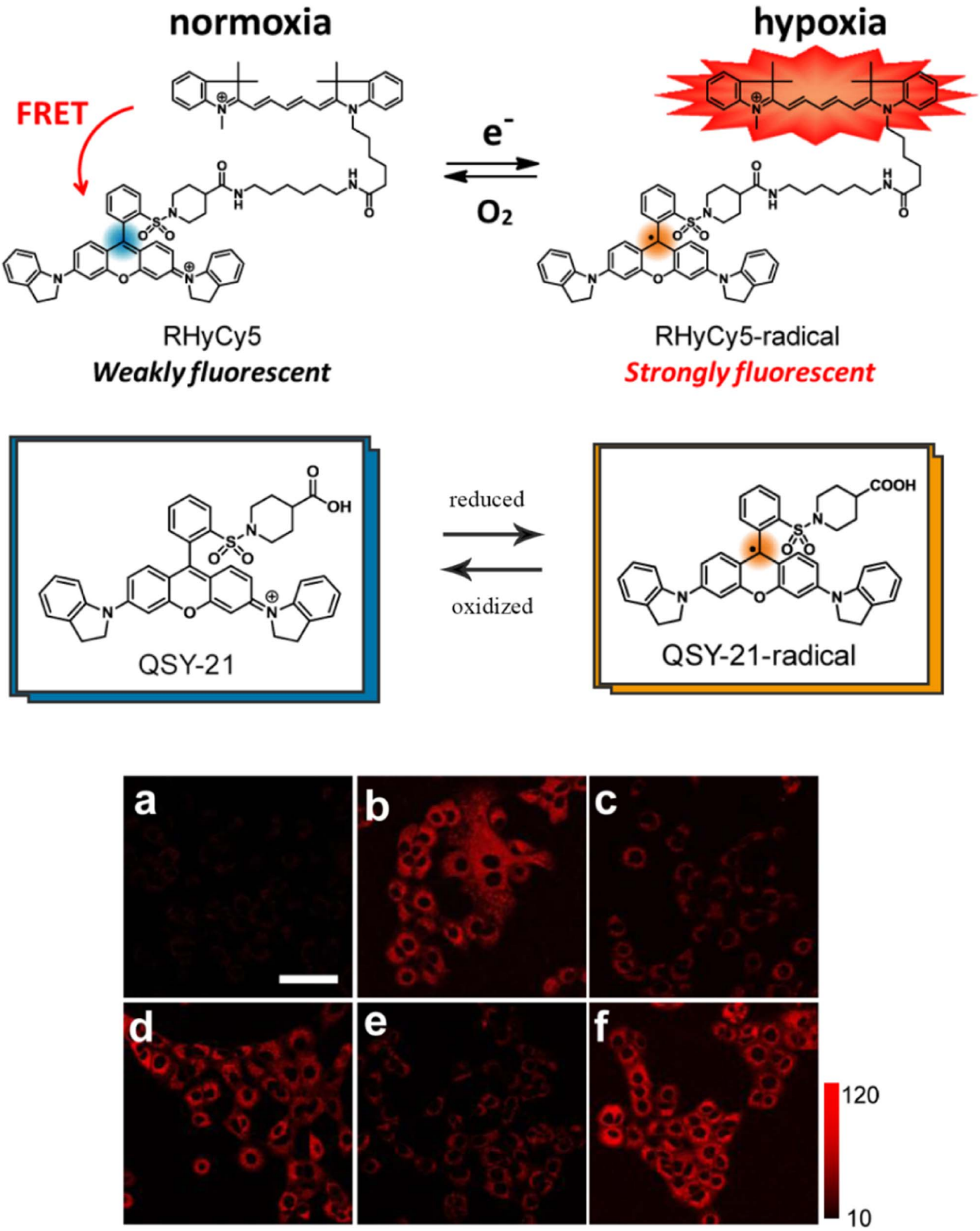

Fig. 6. Biosensor RHyCy5, its FRET acceptor QSY-21 and their reduced radical forms under hypoxia, as well as real-time monitoring of repeated hypoxia-normoxia cycles in A549 cells by fluorescence confocal microscopy [From Takahashi et al. (2012)].

living biological systems. Hence, ROS-responsive biosensors, though not own the high specificity and sensitivity to one individual ROS as the biosensors afore-mentioned, are powerful to disclose the functions and relations of multiple ROS. Two reversible biosensors 2-Me TeR (Koide et al., 2012) and GeP640 (Nie et al., 2016) were developed in Nagano's laboratory and Zhang's laboratory for detecting the redox changes of multiple ROS.

Biosensor 2-Me TeR, in Fig. 7, can effectively detect ·OH, $ONOO^-$ and ^-OCl at once. It was a tellurium-rhodamine-based compound and was synthesized by replacing the O atom of the xanthene moiety of

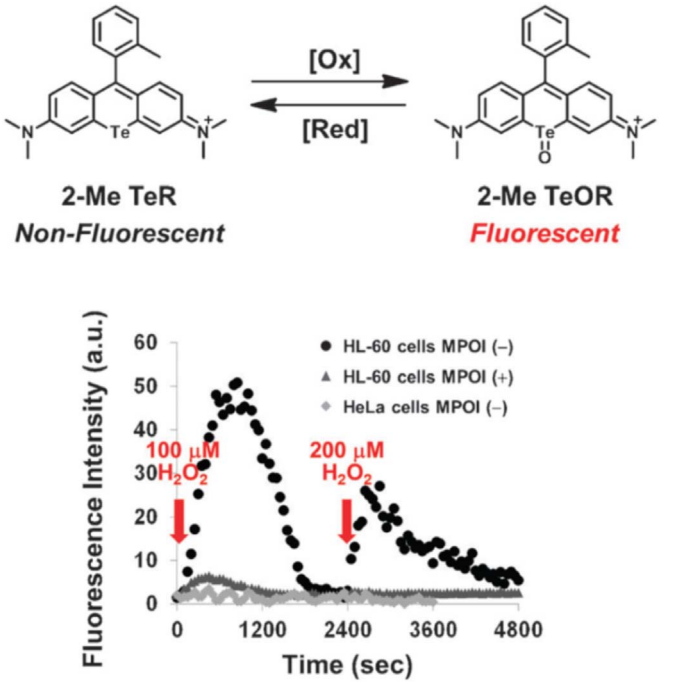

Fig. 7. Biosensor 2-Me TeR, its oxidized product 2-Me TeOR and the time courses of the change in fluorescence intensity for H_2O_2-stimulated and H_2O_2-unstimulated HL-60 cells and H_2O_2-stimulated HeLa cells [From Koide et al. (2012)].

rhodamines with a Te atom. 2-Me TeR showed an absorption maximum at 600 nm and no fluorescence due to heavy atom effect in 2-Me TeR. Upon ROS detection, 2-Me TeR was oxidized to 2-Me TeOR through the selective oxidation of the Te atom. This oxidized product 2-Me TeOR displayed maximum absorption and maximum emission at 669 nm and 686 nm, respectively, and the fluorescence intensity of 2-Me TeOR increased with a factor of ~200-fold upon ROS detection due to that the oxidation of the Te atom has weakened the heavy atom effect in 2-Me TeOR. Applying 2-Me TeR to H_2O_2-stimulated living HL-60 cells which can produce a large amount of ROS (*e.g.*, $^{-}$OCl), the reversible redox cycles of endogenously produced ROS were successfully monitored by the time courses of the change in fluorescent intensity (Fig. 7).

As illustrated in Fig. 8, biosensor GeP640 was based on novel Ge-pyronine dyes (GePs) and was synthesized by the germanium substitution of the O atom of the xanthene moiety of O-pyronine (OP). GeP640 also can effectively detect ·OH, $ONOO^-$ and $^{-}$OCl simultaneously, and it showed maximum adsorption and maximum emission at 621 nm and 643 nm, respectively. Expansion of the xanthene ring can cause the emission wavelength in the NIR region (665 and 682 nm). Upon reaction with GSH, the fluorescence of the biosensor is greatly quenched due to the formation of a nonemissive product and the quenching mechanism is associated with an interruption of $\pi-\pi$ conjugation. GeP640 allowed the real-time imaging of ROS stress and GSH repair in living HL-60 cells under H_2O_2 stimulation with the production of a large amount of ROS (*e.g.* $^{-}$OCl) and the time courses of the change in fluorescence intensity monitored the instantaneous concentration changes of ROS (Fig. 8).

Both sensors showed selectively high sensitivity to ·OH, $ONOO^-$ and $^{-}$OCl against other ROS (H_2O_2, KO_2, ·NO, $O_2^{\cdot -}$). The oxidation-reduction cycles of 2-Me TeR/GeP640 can be repeated at least 3/4 times with a moderate decrease of 20% in fluorescent intensity. GeP640 also features the ultrafast response to ROS/GSH within 20 s/10 s, high fluorescence quantum yield (0.32–0.44) in aqueous media, good cell permeability and low cytotoxicity.

Recently, Chen and coworkers also synthesized a ROS-sensitive NIR ratiometric biosensor Cy-NB (Yin et al., 2015) with cysteine sensitivity for *in vivo* monitoring of mitochondrial oxidative stress. In Cy-NB, heptamethine cyanine dye is acting as the fluorophore and p-nitrobenzoyl as the fluorescent modulator. But they did not refer the reversibility of this biosensor.

7. Design strategy for redox-responsive reversible NIR biosensors

In general, the redox-responsive reversible NIR biosensor consists of NIR fluorophore platform and fluorescent modulator reversibly responsive to ROS and their antioxidants. In recent development of these biosensors in particular with modulators, one primary design strategy is relied on mimicking the GPx activity, where GPx is a selenoenzyme that protects organisms from oxidative damage through catalyzing the reduction of hydroperoxides by glutathione. This primary strategy has been utilized in the design and synthesis of biosensors Cy-PSe, BzSe-Cy, diMPhSe-BOD, Cy-O-Eb, Cy-NTe and 2-Me TeR. Here, either the selenium atom or the tellurium atom is acting as the functional core of the sensing group in these reversible ROS biosensors. In more details, Cy-PSe, BzSe-Cy and diMPhSe-BOD are based on monoselenides and Cy-O-Eb is based on ebselen, and both monoselenides and ebselen are known to be the major GPx mimics (Nascimento et al., 2012); Cy-NTe and 2-Me TeR are based on organotellurium compounds due to some of the organotellurium compounds show even higher GPx-like activity and more remarkable antioxidant ability than their organoselenium analogues (Ba et al., 2010). In addition, for these selenium-based and tellurium-based biosensors, ROS oxidation converted only selenium or tellurium element to its oxide form, and their sensing mechanism is usually associated with the heavy atom effects (diMPhSe-BOD and 2-Me TeR) or with the PET mechanism (others).

Design strategy for Cy-TemOH is based on the nitroxides' reversible response to oxidation and reduction. Specifically, it utilizes the redox couple of hydroxylamine and Oam: ascorbic acid reduced nitroxides to hydroxylamine, and HBrO oxidized hydroxylamine to Oam which then converted back to hydroxylamine with reduction of ascorbic acid (Ishii et al., 2011). Rather similarly, quinones' reversible response to oxidation and reduction, or the utilization of the redox couple of hydroquinone and quinone, offers the strategy to design DA-Cy. In DA-Cy, the redox-active dopamine was attached to a cyanine dye, and ROS oxidation converted the dopamine to DA-o-quinone which was then scavenged by cellular thiols (mainly GSH) through Michael addition to give thiol-DA conjugates (Shen et al., 1996). Other strategies such as the FRET mechanism and the utilization of the novel Ge-pyronine dyes have been utilized in the design of RHyCy5 and GeP640.

On the other hand, cyanine dyes are commonly chosen and used as the NIR fluorophores in most of the biosensors for their NIR emission, high molar absorptivity, low cytotoxicity, ability of subcellular location and good biocompatibility. In addition, BODIPY dyes and Ge-pyronine dyes are also used as the NIR fluorophores of some reversible ROS biosensors.

Fig. 9 demonstrates the design strategies in recent development of the redox-responsive reversible NIR biosensors applicable to *in vitro/in vivo* fluorescence imaging, utilizing the GPx mimics (*e.g.*, organoselenium compounds and organotellurium compounds), the nitroxides, the quinones, the FRET mechanism and the novel GePs.

8. Summary and perspective

In this article, we have surveyed the recently (2011–2016) developed redox-responsive reversible NIR biosensors which have

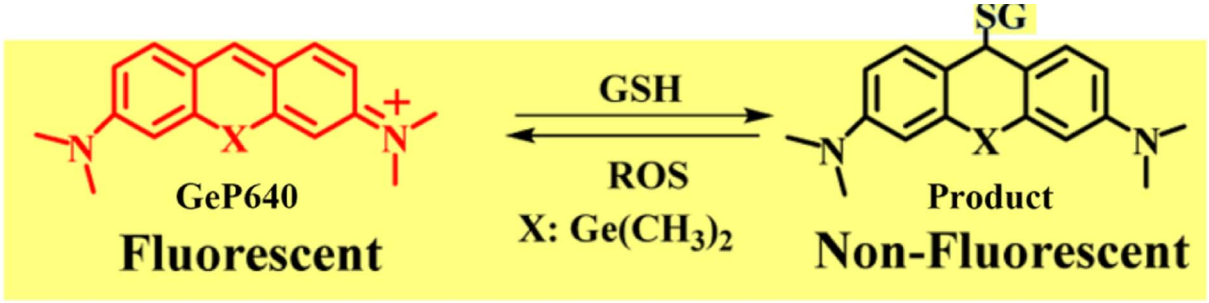

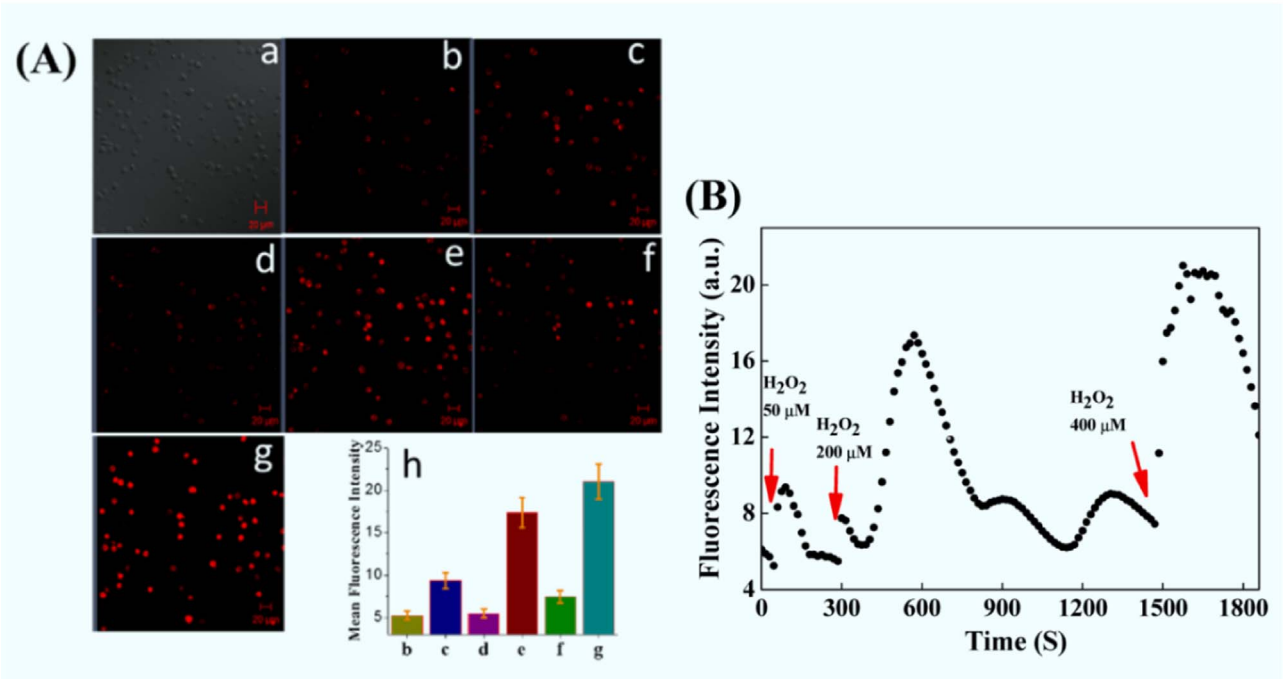

Fig. 8. Biosensor GeP640 and its reduced product, (A) real-time imaging of multiple redox cycles between ROS stress and GSH repair and (B) time courses of the change in fluorescence intensity in living HL-60 cells. [From Nie et al. (2016)].

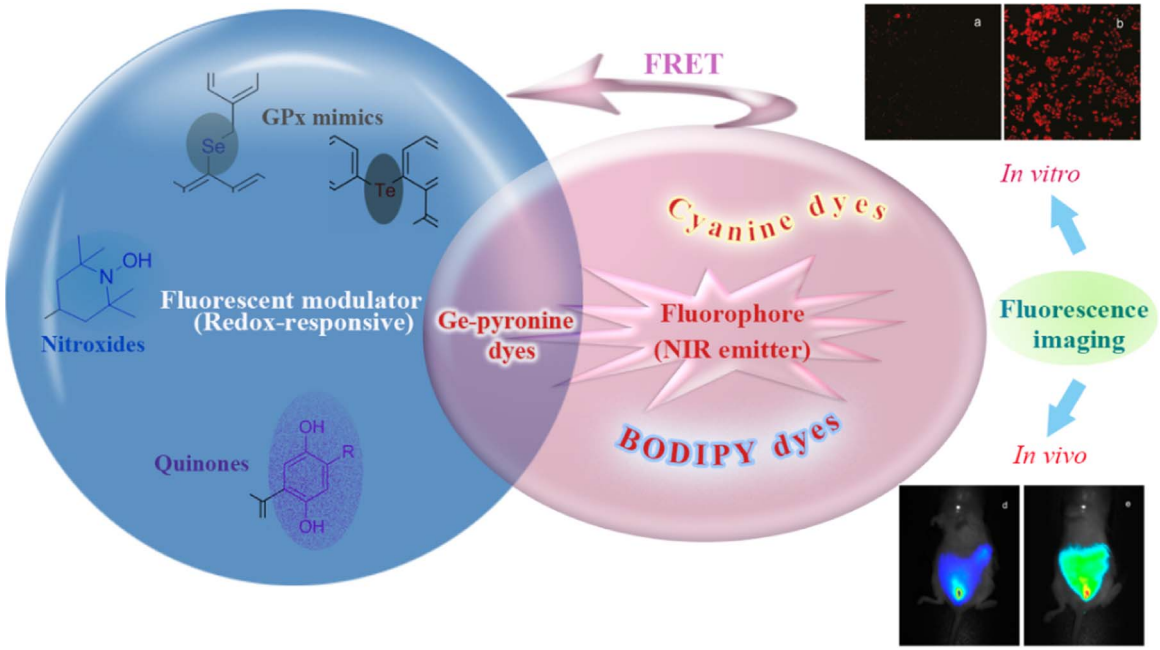

Fig. 9. Design strategies in the recent development of redox-responsive reversible NIR biosensors which allowed for real-time fluorescence imaging of multiple redox cycles in living cells and small animals.

successfully detected the small transient ROS burst and reversibly monitored the oxidation and reduction events in living cells and small animals through *in vitro/in vivo* fluorescence imaging. These small-molecule biosensors, which are most applicable to *in vivo/in vitro* fluorescence imaging and with the capability to dynamically detect the redox changes at cellular level, have the following salient features: NIR absorption and emission; high selectivity and sensitivity to (individual) ROS; quantitative detection of ROS (linear correlation between fluorescence intensity and ROS concentration); high sensitivity or rapid response to (individual) ROS and their antioxidants; reversibility (cycling back and forth through continuous oxidation and reduction); cellular permeability and capability of subcellular localization; tissue penetration; low cytotoxicity; water solubility; minimum effect on cellular homeostasis. In their design strategies, organoselenium and organotellurium compounds mimicking the GPx-like activity, nitroxides and quinones are commonly chosen as the redox-responsive fluorescent modulators, and fluorescence "turn on" or "turn off" is thus triggered by their reversible response to oxidation or to reduction. In mechanism, their fluorescence sensing originates from either the fast PET or the heavy atom effects (organoselenium- and organotellurium-based), d-PET (nitroxides- and quinones-based), FRET (FRET-based), interruption of $\pi-\pi$ conjugation (GePs-based). Up to date, these design strategies and the thus designed biosensors are proved to be successful and significant in sensing the redox status in living biological systems. Most importantly, all these biosensors enabled the successful application in *in vitro* and *in vivo* studies. Table 1 summarizes the features of the redox-responsive reversible NIR small-molecule biosensors in this survey.

Thus far, the *in vitro* and *in vivo* fluorescence imaging with these recent NIR biosensors generally employed only one kind of biosensors specified to one individual ROS. Future experiments could consider using two or more kinds of biosensors in one imaging process. Although this combination of different kinds of biosensors becomes more complicated and is thus difficult to handle, it is more promising for understanding and analyzing biological synergy and dynamical relations between two individual ROS through detecting redox changes with more than one individual ROS involved. Future work could also focus on developing ratiometric type of reversible NIR biosensors (such as diMPhSe-BOD) to achieve high signal-to-noise ratio in monitoring the redox cycles in living systems, because ratiometric biosensors are good at resisting environmental interference. Since two-photon fluorescence microscopy offers the advantages of longer observation time, deeper tissue penetration, less photodamage and local excitation, three-dimensional imaging can be realized with two-photon microscopy. Hence, future attention on developing two-photon ROS biosensors would also have significant implications for the ROS studies with two-photon microscopy. However, quantities of ratiometric biosensors and two-photon biosensors, especially the redox-responsive reversible NIR biosensors, are not many thus far.

There still leaves room for developing new functional organic compounds that contain the organochalcogen atoms and can mimic the GPx-like activity to serve as the redox-responsive fluorescent modulators as well as for proposing new ways to make fluorescence emission in NIR range, such as utilizing the strong electron-donating properties of Se group in the design of diMPhSe-BOD and utilizing the expansion of the xanthene ring in the design of GeP640. Developing new NIR dyes to serve as suitable fluorescent fluorophores is also essential to the future development of redox-responsive reversible NIR biosensors. In particular, since the emission wavelength of 820 nm now seems to be the up bound of the recent redox-responsive reversible NIR biosensors, thus, future extension to even longer wavelength range

Table 1
Features of the redox-responsive reversible NIR small-molecule biosensors.

Biosensor	Excitation (nm)	Emission (nm)	Design strategy	Sensing mechanism	Selectivity	Reversibility (oxidation- reduction cycles)	Subcellular location	Refs
Cy-PSe	758	775–800	Organoselenium compounds (GPx mimics)	PET	$ONOO^-$	5	Mitochondria	Yu et al., 2011
BzSe-Cy	770	795	Organoselenium compounds (GPx mimics)	PET	$ONOO^-$	8	Mitochondria	Xu et al., 2011
Cy-NTe	793	820	Organotellurim compounds (GPx mimics)	PET	$ONOO^-$	5	Mitochondria	Yu et al., 2013
Cy-TemOH	702	755	Nitroxides	d-PET	HBrO	3	Cytoplasm	Yu et al., 2012c
diMPhSe-BOD (Ratiometric type)	610	635, 711	Organoselenium compounds (GPx mimics)	Heavy atom effect	HBrO	5	Cytoplasm	Wang et al., 2013c
DA–Cy	630	755	Quinones	d-PET	H_2O_2	–	Cytoplasm	Yu et al., 2012d
Cy-O-Eb	768	794	Organoselenium compounds (GPx mimics)	PET	H_2O_2	4	Mitochondria	Xu et al., 2013
RHyCy5	660	650	FRET	FRET	O_2	–	–	Takahashi et al., 2012
2-Me TeR	600	686	Organotellurim compounds (GPx mimics)	Heavy atom effect	ROS: $\cdot OH$, $ONOO^-$, ^-OCl	3	–	Koide et al., 2012
GeP640	621	643	GePs	Interruption of $\pi-\pi$ conjugation	ROS: $\cdot OH$, $ONOO^-$, ^-OCl	4	–	Nie et al., 2016

(900–1000 nm) will greatly enhance their potential applications in biological *in vivo* imaging for, *e.g.*, noninvasive and sensitive tumor diagnosis.

Further, elucidation of sensing mechanism is usually facilitated with theoretical investigation. Since the DFT/TD-DFT theoretical approaches have been proved to be very useful for the mechanism studies of molecule sensing systems especially for photophysical or spectroscopic studies (Zhao and Han, 2007a, 2007b, 2008a, 2008b, 2012; Zhao et al., 2007; Chen et al., 2013a, 2013b, 2014a, 2015, 2013c, 2013d, 2014b; Li et al., 2011, 2012; Song et al., 2012a, 2012b; Li and Chu, 2011), they could also be essential to the future design, development, reasoning and understanding of biosensors.

Here, the primary design strategy based on mimicking the GPx-like activity, proposed originally by Han and coworkers in their development of the redox-responsive biosensors, indeed provided a good illumination to the future development of biosensors for detecting biological changes in living systems: the best idea always comes from mimicking functionality of a biological system itself, just like mimicking the catalytic cycle of selenium enzyme with organochalcogen compounds.

Developing NIR biosensors is indispensible to *in vivo* fluorescence bioimaging. The near future will surely see the continued evolution of NIR biosensors, which will be partially benefited from the recent researches on NIR small-molecule biosensors. Finally, we mention that there is still some distance to go to use these NIR small-molecule biosensors in clinic applications and it is necessary to develop flexible and versatile ways, such as using these NIR biosensors as a component of a nanoparticle delivery systems or a self-assembly micelle delivery system (Guo et al., 2014; Woolley et al., 2013), to further improve their stability, reversibility, sensitivity, selectivity, tumor targetability, quick-response ability, anti-interference ability and biocompatibility.

Acknowledgments

The authors acknowledged the financial support from the National Natural Science Foundation of China (NSFC no. 21273234), the Shandong Provincial Natural Science Foundation, China (no. ZR2014AM025), the National Basic Research Program of China (no. 2013CB834604), and the Open Research Fund of the SKLMRD of DICP, China (no. SKLMRD-K201612).

References

Ba, L.A., Doring, M., Jamier, V., Jacob, C., 2010. Org. Biomol. Chem. 8, 4203–4216.
Baker, M., 2010. Nature 463, 977–980.
Balaban, R.S., Nemoto, S., Finkel, T., 2005. Cell 120, 483–495.
Benniston, A.C., Copley, G., Elliott, K.J., Harrington, R.W., Clegg, W., 2008. Eur. J. Org. Chem. 2008, 2705–2713.
Chan, J., Dodani, S.C., Chang, C.J., 2012. Nat. Chem. 4, 973–984.
Chen, J.S., Liu, R.Z., Yang, Y., Chu, T.S., 2013b. Theor. Chem. Acc. 133, 1411.
Chen, J.S., Zhou, P.W., Zhao, L., Chu, T.S., 2014b. RSC Adv. 4, 254–259.
Chen, J.S., Zhao, F.J., Yang, Y., Chu, T.S., 2015. RSC Adv. 5, 36279–36287.
Chen, J.S., Zhao, G.J., Cook, T.R., Han, K.L., Stang, P.J., 2013a. J. AM. Chem. Soc. 135, 6694–6702.
Chen, J.S., Zhou, P.W., Li, G.Y., Chu, T.S., He, G.Z., 2013c. J. Phys. Chem. B 117, 5212–5221.
Chen, J.S., Zhou, P.W., Yang, S.Q., Fu, A.P., Chu, T.S., 2013d. Phys. Chem. Chem. Phys. 15, 16183–16189.
Chen, J.S., Yuan, M.H., Wang, J.P., Yang, Y., Chu, T.S., 2014a. J. Phys. Chem. A 118, 8986–8995.
Chen, X., Zhou, Y., Peng, X., Yoon, J., 2010. Chem. Soc. Rev. 39, 2120–2135.
Dickinson, B.C., Chang, C.J., 2011. Nat. Chem. Biol. 7, 504–511.
Dickinson, B.C., Srilkun, D., Chang, C.J., 2010. Curr. Opin. Chem. Biol. 14, 50–56.
Droge, W., 2002. Physiol. Rev. 82, 47–95.
Finkel, T., 2011. J. Cell Biolog. 194, 7–15.
Fruehauf, J.P., Meyskens Jr., F.L., 2007. Clin. Cancer Res. 13, 789–794.
Gunnlaugsson, T., Glynn, M., Tocci, G.M., Kruger, P.E., Pfeffer, F.M., 2006. Coord. Chem. Rev. 250, 3094–3117.
Guo, Z., Park, S., Yoon, J., Shin, I., 2014. Chem. Soc. Rev. 43, 16–29.
Hirosawa, S., Arai, S., Takeoka, S., 2012. Chem. Commun. 48, 4845–4847.
Ishii, K., Kubo, K., Sakurada, T., Komori, K., Sakai, Y., 2011. Chem. Commun. 47, 4932–4934.
Kierat, R.M., Thaler, B.M., Kramer, R., 2010. Bioorg. Med. Chem. Lett. 20, 1457–1459.
Koide, Y., Kawaguchi, M., Urano, Y., Hanaoka, K., Komatsu, T., Abo, M., Terai, T., Nagano, T., 2012. Chem. Commun. 48, 3091–3093.
Kundu, K., Knight, S.F., Willett, N., Lee, S., Taylor, W.R., Murthy, N., 2009. Angew. Chem. 48, 299–303.
Kurishita, Y., Kohira, T., Ojida, A., Hamachi, I., 2010. J. Am. Chem. Soc. 132, 13290–13299.
Li, D., Wang, Y., Han, K., 2012. Coord. Chem. Rev. 256, 1137–1150.
Li, D., Huang, X., Han, K., Zhan, C.-G., 2011. J. Am. Chem. Soc. 133, 7416–7427.
Li, G.Y., Chu, T.S., 2011. Phys. Chem. Chem. Phys. 13, 20766–20771.
Li, X., Tao, R.R., Hong, L.J., Cheng, J., Jiang, Q., Lu, Y.M., Liao, M.H., Ye, W.F., Lu, N.N., Han, F., Hu, Y.Z., Hu, Y.H., 2015. J. AM. Chem. Soc. 137, 12296–12303.
Liu, S.R., Wu, S.P., 2013. Org. Lett. 15, 878–881.
Lou, Z., Li, P., Han, K., 2015. Acc. Chem. Res. 48, 1358–1368.
Lou, Z., Li, P., Pan, Q., Han, K., 2013a. Chem. Commun. 49, 2445–2447.
Lou, Z., Li, P., Song, P., Han, K., 2013c. Analyst 138, 6291–6295.
Lou, Z., Yang, S., Li, P., Zhou, P., Han, K., 2014. Phys. Chem. Chem. Phys. 16, 3749–3756.
Lou, Z., Li, P., Sun, X., Yang, S., Wang, B., Han, K., 2013b. Chem. Commun. 49, 391–393.
Lu, T., Pan, Y., Kao, S. -Y., Li, C., Kohane, I., Chan, J., Yankner, B.A., 2004. Nature 429, 883–891.
Manjare, S.T., Kim, Y., Churchill, D.G., 2014c. Acc. Chem. Res. 47, 2985–2998.
Manjare, S.T., Kim, S., Heo, W.D., Churchill, D.G., 2014a. Org. Lett. 16, 410–412.
Manjare, S.T., Kim, J., Lee, Y., Churchill, D.G., 2014b. Org. Lett. 16, 520–523.
Miller, E.W., Bian, S.X., Chang, C.J., 2007. J. Am. Chem. Soc. 129, 3458–3459.
Narayanaswamy, N., Narra, S., Nair, R.R., Saini, D.K., Kondaiah, P., Govindaraju, T., 2016. Chem. Sci. 7, 2832–2841.
Nascimento, V., Alberto, E.E., Tondo, D.W., Dambrowski, D., Detty, M.R., Nome, F., Braga, A.L., 2012. J. Am. Chem. Soc. 134, 138–141.
Nie, H., Jing, J., Tian, Y., Yang, W., Zhang, R., Zhang, X., 2016. ACS Appl. Mater. Interfaces 8, 8991–8997.
Que, E.L., Domaille, D.W., Chang, C.J., 2008. Chem. Rev. 108, 1517–1549.
Rao, J., Dragulescu-Andrasi, A., Yao, H., 2007. Curr. Opin. Biotechnol. 18, 17–25.
Reddie, K.G., Humphries, W.H., Bain, C.P., Payne, C.K., Kemp, M.L., Murthy, N., 2012. Org. Lett. 14, 680–683.
Schulz, J.B., Lindenau, J., Seyfried, J., Dichgans, J., 2000. Eur. J. Biochem. 267, 4904–4911.
Shahrokhian, S., 2001. Anal. Chem. 73, 5972–5978.
Shen, X., Xia, B., Wrona, M.Z., Dryhurst, G., 1996. Chem. Res. Toxicol. 9, 1117–1126.
Song, P., Ding, J.X., Chu, T.S., 2012b. Spectrochim. Acta A: Mol. Biomol. Spectr. 97, 746–752.
Song, P., Gao, A.H., Zhou, P.W., Chu, T.S., 2012a. J. Phys. Chem. A 116, 5392–5397.
Takahashi, S., Piao, W., Matsumura, Y., Komatsu, T., Ueno, T., Terai, T., Kamachi, T., Kohno, M., Nagano, T., Hanaoka, K., 2012. J. Am. Chem. Soc. 134, 19588–19591.
Wang, B., Yu, F., Li, P., Sun, X., Han, K., 2013b. Dyes Pigments 96, 383–390.
Wang, B., Li, P., Yu, F., Chen, J., Qu, Z., Han, K., 2013c. Chem. Commun. 49, 5790–5792.
Wang, B., Li, P., Yu, F., Song, P., Sun, X., Yang, S., Lou, Z., Han, K., 2013a. Chem. Commun. 49, 1014–1016.
Wardman, P., 2007. Free Radical Biol. Med. 43, 995–1022.
Woolley, J.F., Stanicka, J., Cotter, T.G., 2013. Trends Biochem. Sci. 38, 556–565.
Wu, G., 2010. Adv. Nutr. 1, 31–37.
Xu, K., Chen, H., Tian, J., Ding, B., Xie, Y., Qiang, M., Tang, B., 2011. Chem. Commun. 47, 9468–9470.
Xu, K., Qiang, M., Gao, W., Su, R., Li, N., Gao, Y., Xie, Y., Kong, F., Tang, B., 2013. Chem. Sci. 4, 1079–1086.
Yamada, Y., Tomiyama, Y., Morita, A., Ikekita, M., Aoki, S., 2008. Chembiochem 9, 853–856.
Yang, Y., Zhao, Q., Feng, W., Li, F., 2013. Chem. Rev. 113, 192–270.
Yap, Y.W., Whiteman, M., Cheung, N.S., 2007. Cell. Signaling 19, 219–228.
Yin, K., Yu, F., Zhang, W., Chen, L., 2015. Biosen. Bioelectron. 74, 156–164.
Yu, F., Li, P., Wang, B., Han, K., 2013. J. Am. Chem. Soc. 135, 7674–7680.
Yu, F., Song, P., Li, P., Wang, B., Han, K., 2012a. Analyst 137, 3740–3749.
Yu, F., Song, P., Li, P., Wang, B., Han, K., 2012c. Chem. Commun. 48, 7735–7737.
Yu, F., Li, P., Li, G., Zhao, G., Chu, T., Han, K., 2011. J. Am. Chem. Soc. 133, 11030–11033.
Yu, F., Li, P., Song, P., Wang, B., Zhao, J., Han, K., 2012b. Chem. Commun. 48, 2852–2854.
Yu, F., Li, P., Song, P., Wang, B., Zhao, J., Han, K., 2012d. Chem. Commun. 48, 4980–4982.
Zhang, W., Li, P., Yang, F., Hu, X., Sun, C., Zhang, W., Chen, D., Tang, B., 2013. J. Am. Chem. Soc. 135, 14956–14959.
Zhao, G.J., Han, K.L., 2007a. J. Phys. Chem. 111, 2469–2474.
Zhao, G.J., Han, K.L., 2007b. J. Phys. Chem. 111, 9218–9223.
Zhao, G.J., Han, K.L., 2008a. Biophys. J. 94, 38–46.
Zhao, G.J., Han, K.L., 2008b. Chemphyschem 9, 1842–1846.
Zhao, G.J., Han, K.L., 2012. Acc. Chem. Res. 45, 404–413.
Zhao, G.J., Liu, J.Y., Zhou, L.C., Han, K.L., 2007. J. Phys. Chem. B 111, 8940–8945.